UWB for Robust Indoor Tracking: Weighting of Multipath Components for Efficient Estimation

Paul Meissner, Erik Leitinger, and Klaus Witrisal

***Abstract*—In a radio propagation channel, deterministic reflections carry important position-related information. With the help of prior knowledge such as a floor plan, this information can be exploited for indoor localization. This letter presents the improvement of a multipath-assisted tracking approach using information about the relevance of deterministic multipath components in an environment. This information is fed to a tracking filter as observation noise model. It is estimated from a few training signals between anchors and an agent at known positions. Tracking results are presented for measurements in a partial non-line-of-sight environment. At a bandwidth of 2 GHz, an accuracy of 4 cm can be achieved for over 90 % of the positions if additional channel information is available. Otherwise, this accuracy is only possible for about 45 % of the positions. The covariance of the estimation matches closely to the corresponding Cramèr-Rao Lower Bound.**

I. Introduction

Robustness and accuracy are key requirements of indoor localization systems. We define robustness as the percentage of cases in which a system can achieve its given potential accuracy. Due to their fine time resolution, range-based ultra-wideband (UWB) systems provide accurate distance estimates between anchors and the agent to be localized [1]. However, a non-line-of-sight (NLOS) situation can decrease the robustness due to biased range estimates. We have proposed an approach called multipath-assisted indoor navigation and tracking (MINT) to enhance the robustness [2], [3]. It makes use of the floor plan to associate multipath components (MPCs) to the surrounding geometry.

In this paper, we show how position-related information can be used efficiently as additional prior information. Channel parameters describing the reliability of the reflected MPCs [3], [4] are estimated from a few training signals with an agent at known positions and used in the tracking filter as measurement noise model. For a navigating agent, awareness to the uncertainty of the available information is crucial for the tracking performance both in theoretic [5] and in practical settings [6]. Taking into account diffuse multipath (DM) allows for much more realistic performance indications [7], especially in dense multipath environments.

The main contributions of this letter are:

- We show that a multipath-assisted tracking approach can be made aware of the relevance of specific deterministic MPCs in an environment.
- Using measurements, we show that centimeter-level accuracy can be achieved robustly also in NLOS conditions.

P. Meissner, E. Leitinger and K. Witrisal are with Graz University of Technology, Graz, Austria, email: paul.meissner@tugraz.at.

The authors thank Manuel Lafer for his help in performing the measurements.

Notation: The symbols $*$, $(\cdot)^T$, $(\cdot)^*$, $\mathbb{E}\{\cdot\}$, $\Re\{\cdot\}$, and $\mathbf{I}_N$ denote convolution, transposition, conjugation, expectation, real part, and an identity matrix of dimension N, respectively.

II. Tracking and Channel Estimation

A. Signal and Geometry Models

We aim at tracking a mobile agent in an environment with J anchors at known positions. The signal between the j-th anchor and the agent at the position $\mathbf{p}_\ell$ is modeled as [3]

$$r_\ell^{(j)}(t) = \sum_{k=1}^{K_\ell^{(j)}} \alpha_{k,\ell}^{(j)} s(t-\tau_{k,\ell}^{(j)}) + s(t) * \nu_\ell^{(j)}(t) + w(t). \quad (1)$$

The sets $\{\alpha_{k,\ell}^{(j)}\}$ and $\{\tau_{k,\ell}^{(j)}\}$ are the complex amplitudes and delays of the k-th deterministic MPC, respectively. The signal $s(t)$ denotes the transmitted pulse shape with effective pulse duration T_p. The random process $\nu_\ell^{(j)}(t)$ denotes DM and is modeled as a Gaussian process with auto-covariance $\mathbb{E}\{\nu_\ell^{(j)}(\tau)[\nu_\ell^{(j)}(u)]^*\} = S_{\nu,\ell}^{(j)}(\tau)\delta(\tau-u)$, where $S_{\nu,\ell}^{(j)}(\tau)$ is the power delay profile (PDP) of the DM. The signal $w(t)$ denotes white Gaussian measurement noise with double-sided power spectral density (PSD) of $N_0/2$.

The delays of the $K_\ell^{(j)}$ deterministic MPCs are modeled geometrically using mirror images of the j-th anchor with respect to the corresponding walls, introducing so-called virtual anchors (VAs) [2], [8]. Fig. 1 shows two examples of such VAs. It can be seen that the distance from the agent's position $\mathbf{p}_\ell$ to the k-th VA at $\mathbf{a}_k^{(j)}$ corresponds to the delay $\tau_{k,\ell}^{(j)} = \frac{1}{c} d_{k,\ell}^{(j)} = \frac{1}{c}\|\mathbf{p}_\ell - \mathbf{a}_k^{(j)}\|$ of the corresponding MPC, where c denotes the speed of light. For the whole scenario, a set $\mathcal{A}^{(j)}$ of all potential VAs of the j-th anchor can be constructed. Higher-order VAs are obtained by mirroring again lower-order VAs with respect to reflectors. Using optical ray-tracing, the set of visible VAs can be computed for position $\mathbf{p}_\ell$ as

$$\mathcal{A}_\ell^{(j)} = \{\mathbf{a}_{\ell,1}^{(j)}, \ldots, \mathbf{a}_{\ell,K_\ell^{(j)}}^{(j)}\} = \{\mathbf{a}_k^{(j)} : f_\mathrm{vis}(\mathbf{a}_k^{(j)}, \mathbf{p}_\ell) = 1\} \quad (2)$$

where the ray-tracing is expressed by the function

$$f_\mathrm{vis}(\mathbf{a}_k^{(j)}, \mathbf{p}) = \begin{cases} 1, & \text{if VA } \mathbf{a}_k^{(j)} \text{ is visible at } \mathbf{p} \\ 0, & \text{else.} \end{cases} \quad (3)$$

B. Tracking Algorithm

In a first step, the location-dependent parameters, i.e. the arrival times of the deterministic MPCs, are estimated from the received signal modeled by (1). The arrival time estimation

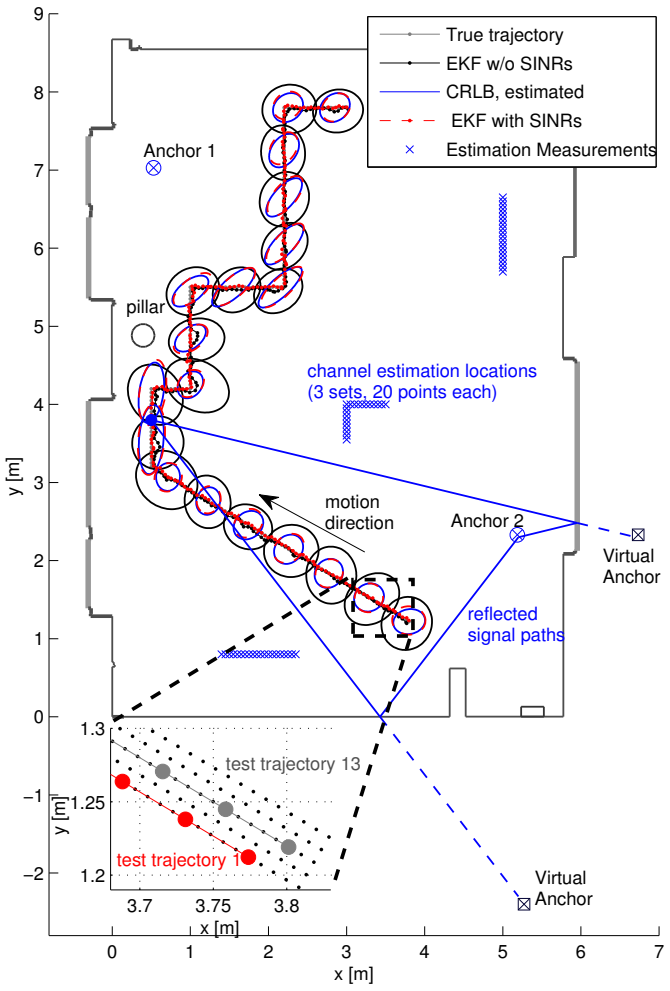

Fig. 1. Floor plan of the evaluation scenario, bold gray lines denote windows and other lines illustrate walls made of different materials. Examples for true and estimated agent trajectories are shown, the former is hidden beneath the others. The bottom contains a close-up of the trajectories, illustrating the 1-cm-spaced grid, out of which 25 5-cm-spaced trajectories are obtained. Two physical anchors are indicated with examples for virtual anchors modeling reflections from walls. Ellipses denote 20-fold standard deviations of the trackers as well as the respective 20-fold CRLB, as described in the text.

at position ℓ is realized as an iterative least-squares approximation of the received signal

$$\hat{\tau}_{k,\ell}^{(j)} = \arg\min_{\tau} \int_0^T \left| r_\ell^{(j)}(t) - \hat{r}_{\ell,k-1}^{(j)}(t) - \hat{\alpha}(\tau) s(t-\tau) \right|^2 dt \tag{4}$$

using a template signal $\hat{r}_{\ell,k}^{(j)}(t) = \sum_{k'=1}^{k} \hat{\alpha}_{k',\ell}^{(j)} s(t - \hat{\tau}_{k',\ell}^{(j)})$ for all MPCs up to the k-th. The path amplitudes are nuisance parameters, estimated using a projection of $r_\ell^{(j)}(t)$ onto a unit energy pulse $s(t)$ as

$$\hat{\alpha}(\tau) = \int_0^T [r_\ell^{(j)}(t)]^* s(t-\tau) dt; \quad \hat{\alpha}_{k,\ell}^{(j)} = \hat{\alpha}(\hat{\tau}_{k,\ell}^{(j)}). \tag{5}$$

The number of estimated MPCs $\hat{K}_\ell^{(j)}$ should be chosen according to the number of expected specular paths in an environment. With the assumptions of separable MPCs and white noise, (4) and (5) correspond to a maximum-likelihood (ML) estimation of the deterministic MPCs.

The tracking is done as in [2] using an EKF with data association (DA), which is necessary since the estimated MPC arrival times in (4) are not associated to the VAs. We choose a simple linear Gaussian constant-velocity motion model

$$\begin{aligned} \mathbf{x}_{\ell+1} =& \mathbf{F}\mathbf{x}_\ell + \mathbf{G}\mathbf{n}_{\mathrm{a},\ell} \\ =& \begin{bmatrix} 1 & 0 & \Delta T & 0 \\ 0 & 1 & 0 & \Delta T \\ 0 & 0 & 1 & 0 \\ 0 & 0 & 0 & 1 \end{bmatrix} \mathbf{x}_\ell + \begin{bmatrix} \frac{\Delta T^2}{2} & 0 \\ 0 & \frac{\Delta T^2}{2} \\ \Delta T & 0 \\ 0 & \Delta T \end{bmatrix} \mathbf{n}_{\mathrm{a},\ell}. \end{aligned} \tag{6}$$

The state vector $\mathbf{x}_\ell$ of the agent contains position $\mathbf{p}_\ell$ and the velocity vector, and ΔT is the update rate. The driving acceleration noise term $\mathbf{n}_{\mathrm{a},\ell}$ with zero mean and covariance matrix $\mathbf{Q} = \sigma_a^2 \mathbf{G}\mathbf{G}^T$ models motion changes that deviate from the constant-velocity assumption.

For the measurement update of the EKF, the set of expected VAs is calculated for the DA at the predicted position $\mathbf{p}_\ell^-$ using (2) for each anchor, yielding sets $\bar{\mathcal{A}}_\ell^{(j)}$. At this time, prior information such as a set $\tilde{\mathcal{A}}^{(j)}$ defining *relevant* VAs can be used to restrict the set of expected VAs, resulting in $\bar{\mathcal{A}}_\ell^{(j)} \cap \tilde{\mathcal{A}}^{(j)}$. The corresponding expected path delays are then matched to the estimated arrival times (4) such that the cumulative distance of estimated and expected delays is minimized, yielding sets of associated VAs $\mathcal{A}_{\ell,\mathrm{ass}}^{(j)}$. The association is done using a constrained optimal subpattern assignment approach [2], [9], where the constraint is that associations at a distance larger than a given maximum ranging uncertainty, the so-called cut-off distance d_c, are discarded.

After joining information from all anchors, $\mathcal{A}_{\ell,\mathrm{ass}} = \bigcup_j \mathcal{A}_{\ell,\mathrm{ass}}^{(j)}$, the corresponding distance estimates are stacked in the EKF's measurement input vector which is *modeled* as

$$\mathbf{z}_\ell = \left[\ldots, \ \|\mathbf{a}_k^{(j)} - \mathbf{p}_\ell\|, \ \ldots \right]^T + \mathbf{n}_{z,\ell}, \ \mathbf{a}_k^{(j)} \in \mathcal{A}_{\ell,\mathrm{ass}}. \tag{7}$$

The measurement noise $\mathbf{n}_{z,\ell}$ is assumed to be zero-mean multivariate Gaussian. The choice of the measurement noise covariance matrix $\mathbf{R}_\ell$ depends on the amount of prior information. If a-priori estimates of the range estimation uncertainties $\mathrm{var}\left\{\hat{d}_{k,\ell}^{(j)}\right\}$ are available for a set of VAs, then

$$\mathbf{R}_\ell = \mathrm{diag}\left\{ \mathrm{var}\left\{ \hat{d}_{k,\ell}^{(j)} \right\} \right\} \quad \forall\, k,j : \mathbf{a}_k^{(j)} \in \mathcal{A}_{\ell,\mathrm{ass}}. \tag{8}$$

Otherwise, an overall uncertainty σ_d^2 is used, i.e.

$$\mathbf{R}_\ell = \sigma_\mathrm{d}^2 \mathbf{I}_{|\mathcal{A}_{\ell,\mathrm{ass}}|}. \tag{9}$$

C. Position-Related Information and its Estimation

In [3], we have derived the Cramèr Rao Lower Bound (CRLB) for positioning based on the signal model (1) and the VAs. With the assumption of no path overlap, i.e. the MPCs are orthogonal, the equivalent Fisher information matrix (EFIM) for position $\mathbf{p}_\ell$ [10] is given as

$$\mathbf{J}_{\mathbf{p}_\ell} = \sum_{j=1}^{J} \sum_{k=1}^{K_\ell^{(j)}} \mathrm{J}_r(d_{k,\ell}^{(j)}) \mathbf{J}_r(\phi_{k,\ell}^{(j)}). \tag{10}$$

where the ranging direction matrix $\mathbf{J}_r(\phi_{k,\ell}^{(j)})$ determines the direction $\phi_{k,\ell}^{(j)}$ of the information of the k-th MPC, since it

is spanned by the outer product of the unit vector pointing from the k-th VA at $\mathbf{a}_k^{(j)}$ to the agent at $\mathbf{p}_\ell$ with itself [3]. It is scaled by the Fisher information contained in the signal $r_\ell^{(j)}(t)$ about the path length $d_{k,\ell}^{(j)}$. Its inverse is the CRLB for the variance of an unbiased range estimate $\hat{d}_{k,\ell}^{(j)}$

$$\mathrm{J}_r^{-1}(d_{k,\ell}^{(j)}) = \left(\frac{8\pi^2\beta^2}{c^2}\mathrm{SINR}_{k,\ell}^{(j)}\right)^{-1} \leq \mathrm{var}\left\{\hat{d}_{k,\ell}^{(j)}\right\}. \quad (11)$$

Here, β denotes the effective (root mean square) bandwidth of $s(t)$ and the signal-to-interference-and-noise-ratio (SINR) of the k-th MPC at $\mathbf{p}_\ell$ is defined as

$$\mathrm{SINR}_{k,\ell}^{(j)} = \frac{|\alpha_{k,\ell}^{(j)}|^2}{N_0 + T_\mathrm{p} S_{\nu,\ell}^{(j)}(\tau_{k,\ell}^{(j)})}. \quad (12)$$

In [4], we have derived an estimator for the average $\mathrm{SINR}_k^{(j)}$, averaged over positions within a confined spatial region in which propagation characteristics such as the PDP of the DM are assumed to be stationary. However, there is only a limited number of MPCs visible within such a region. To increase this number, we use measurements at N_s sets of points $\{\mathbf{p}_\ell : \ell \in \mathcal{P}_i\}$, where $\mathcal{P}_i,\ i = 1, \ldots, N_\mathrm{s}$, collects the indices of the points. Within each set, propagation characteristics are again assumed to be stationary and an $\widehat{\mathrm{SINR}}_k^{(j,i)}$ can be estimated. For this, we have to take into account the *observability* of the corresponding VA. We define the subsets

$$\begin{aligned}\mathcal{P}_k^{(j,i)} =& \{\ell \in \mathcal{P}_i : f_\mathrm{vis}(\mathbf{p}_\ell, \mathbf{a}_k^{(j)}) = 1 \wedge \\ & |\tau_{k,\ell}^{(j)} - \tau_{k',\ell}^{(j)}| > T_\mathrm{p}\ \forall\ k' \neq k,\ \mathbf{a}_{k'}^{(j)} \in \mathcal{A}_\ell^{(j)}\}\end{aligned} \quad (13)$$

with cardinality $N_k^{(j,i)}$. The conditions in (13) imply that the k-th VA is visible at $\mathbf{p}_\ell$ and there is no path overlap [3], [10] with any other VA-modeled MPC.

The overall aim is to take into account the uncertainty of the MPCs in an environment, both w.r.t. the path length estimation and also w.r.t. the position of the VAs, as these are subject to floor plan uncertainties. For the estimation of a *global* range uncertainty of a specific MPC, which is necessary to be useful as a location-independent noise model (8), we propose the weighted mean of the local uncertainties

$$\widehat{\mathrm{var}}\left\{\hat{d}_k^{(j)}\right\} = \frac{1}{\sum_{i=1}^{N_\mathrm{s}} N_k^{(j,i)}} \sum_{i=1}^{N_\mathrm{s}} N_k^{(j,i)} \widehat{\mathrm{var}}\left\{\hat{d}_{k,\ell}^{(j)} : \ell \in \mathcal{P}_k^{(j,i)}\right\}. \quad (14)$$

The $\widehat{\mathrm{var}}\left\{\hat{d}_{k,\ell}^{(j)}\right\}$ is obtained from an SINR estimate and (11). This and the use of (14) are motivated by assuming the range estimates $\hat{d}_{k,\ell}^{(j)}$ to be Gaussian distributed, which is justified by the fact that (4) is an approximation for the according ML estimator and as such is asymptotically efficient, i.e. $\hat{d}_{k,\ell}^{(j)} \sim \mathcal{N}\left(d_{k,\ell}^{(j)}; \mathrm{J}_r^{-1}(d_{k,\ell}^{(j)})\right)$.

The VA positions are corrected using a prior $p(\tilde{\mathbf{a}}_k^{(j)})$ for the k-th VA. This leads to the MAP estimate

$$\hat{\mathbf{a}}_k^{(j)} = \arg\max_{\tilde{\mathbf{a}}_k^{(j)}} \ln p(\mathbf{r}^{(j)}(t)|\tilde{\mathbf{a}}_k^{(j)}) + \ln p(\tilde{\mathbf{a}}_k^{(j)}) \quad (15)$$

with a likelihood function that evaluates the contribution of the k-th VA to all estimation signals $\mathbf{r}^{(j)}(t)$ (c.f. [3] but neglecting the whitening to account for the DM)

$$\begin{aligned}\ln p(\mathbf{r}^{(j)}(t)|\tilde{\mathbf{a}}_k^{(j)}) \propto & \frac{2}{N_0} \sum_{i=1}^{N_\mathrm{s}} \sum_{\ell \in \mathcal{P}_k^{(j,i)}} \int_0^T \Re\left\{[r_\ell^{(j)}(t)]^* \tilde{s}_{k,\ell}^{(j)}(t)\right\} dt \\ & - \frac{1}{N_0} \int_0^T |\tilde{s}_{k,\ell}^{(j)}(t)|^2 dt.\end{aligned} \quad (16)$$

Here, $\tilde{s}_{k,\ell}^{(j)}(t) = \tilde{\alpha}_{k,\ell}^{(j)} s(t - \tilde{\tau}_{k,\ell}^{(j)})$ is a template signal where $\tilde{\tau}_{k,\ell}^{(j)} = \frac{1}{c}\|\tilde{\mathbf{a}}_k^{(j)} - \mathbf{p}_\ell\|$ and the MPC amplitudes are again nuisance parameters and estimated using (5). The vector of received signals for the estimation is given as

$$\mathbf{r}^{(j)}(t) = [r_{\ell\in\mathcal{P}_1}^{(j)}(t),\ \ldots,\ r_{\ell\in\mathcal{P}_{N_\mathrm{s}}}^{(j)}(t)]^T. \quad (17)$$

With the signal model in (1) and $\hat{m}_{1,k}^{(j,i)}$ and $\hat{m}_{2,k}^{(j,i)}$ denoting estimates of the first and second central moments of the energy samples $|\tilde{\alpha}_{k,\ell}^{(j)}|^2$ for $\ell \in \mathcal{P}_k^{(j,i)}$, the corresponding average SINRs are estimated as [4]

$$\widehat{\mathrm{SINR}}_k^{(j,i)} = \left(\frac{\hat{m}_{1,k}^{(j,i)}}{\sqrt{\hat{m}_{1,k}^{(j,i)^2} - \hat{m}_{2,k}^{(j,i)}}} - 1\right)^{-1}. \quad (18)$$

Those can be used together with (11) and (14) to obtain a range uncertainty for the k-th VA for the given environment.

The SINR estimation described in [4] also performs a correction of deterministic factors such as distance-dependent path-loss. Overall, it leads to sets $\tilde{\mathcal{A}}^{(j)}$ of VAs with lower cardinality than $\mathcal{A}^{(j)}$, consisting of re-estimated VA locations obtained in (15).

III. Measurement Scenario

Measurements were obtained along a trajectory of 220 points, spaced by 5 cm, see Fig. 1. Around each point, 25 measurements were performed within a 5 x 5 cm grid, yielding in fact 25 parallel trajectories for the performance analysis.

The channel between the agent on the trajectory and two anchors (see Fig. 1) has been measured with an M-sequence based UWB channel sounder developed by *Ilmsens*, as also described in [11]. On anchor and agent sides, dipole-like antennas made of Euro-cent coins have been used. They have an approximately uniform radiation pattern in azimuth plane and zeroes in the directions of floor and ceiling. Out of the measured frequency range of $3.1 - 10.6$ GHz, a subband with center frequency f_c and bandwidth $B = 1/T_\mathrm{p}$ has been selected using filtering with a raised-cosine pulse $s(t)e^{j2\pi f_\mathrm{c} t}$ with pulse duration T_p, followed by a downconversion.

IV. Results

For the tracking along the 25 trajectories, a frequency range corresponding to $f_\mathrm{c} = 7$ GHz and $T_\mathrm{p} = 0.5$ ns has been chosen, which results in a bandwidth of 2 GHz. The process noise variance in the motion model (6) is obtained as in [2] based on selecting a maximum velocity in e.g. the x-direction $v_{x,\max}$, which defines the 3σ point of the noise in velocity domain. The corresponding process noise variance in the acceleration domain is then $\sigma_a^2 = (v_{x,\max}/(3\Delta T))^2$ with $v_{x,\max} = 1$ m/s and $\Delta T = 1$ s in this paper. The DA cutoff distance has been chosen as $d_\mathrm{c} = 0.12$ m. VAs up to order two

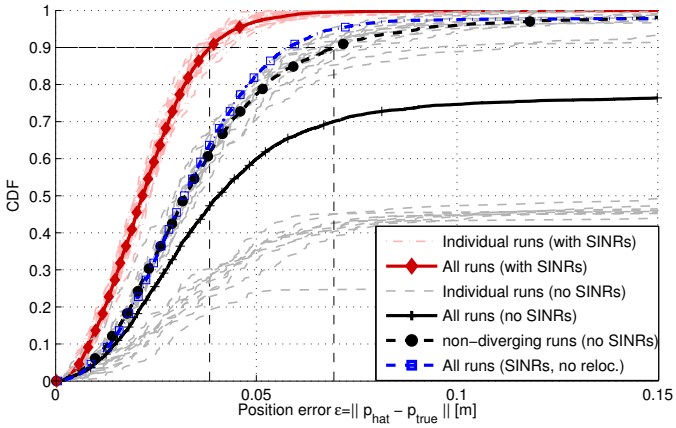

Fig. 2. Performance CDFs for $T_\mathrm{p} = 0.5\,\mathrm{ns}$ and $f_\mathrm{c} = 7\,\mathrm{GHz}$. Thin lines show the individual 25 runs over the trajectories in Fig. 1. Red and gray indicate the EKFs with and without estimated SINRs. Bold lines denote the total performance for all runs, the dashed black line indicates the performance without SINRs on all non-diverging runs (15 out of 25).

have been used, and SINR estimation was done using $N_\mathrm{s} = 3$ sets of 20 points (Fig. 1). The prior for the VA positions in (15) has been chosen as a uniform distribution within a circle of diameter $10\,\mathrm{cm}$ around the calculated VA position. The performance of the EKF is compared for the cases with estimated SINRs (8), and where no such information is available (9). To allow for a fair comparison in the latter case, the overall ranging uncertainty is selected as the mean of the estimated uncertainties, which is $\sigma_\mathrm{d} = 0.042\,\mathrm{m}$.

An exemplary tracking result is illustrated in Fig. 1. In this case, the EKF can track the agent with and without estimated MPC SINRs, also in the NLOS region with respect to Anchor 1 (caused by the concrete pillar on the left side of the room). At every 12-th position, the 20-fold estimation error standard deviation ellipse of the EKF is illustrated. The comparison with the estimated CRLB, given as the inverse of (10), shows a close match to the tracking performance when using the SINRs, which confirms the efficient use of the MPCs. It should be noted that the CRLB shown does not include the motion model, i.e. it is not the posterior CRLB. However, for the chosen process noise variance, which is deliberately larger than the measurement uncertainties, the motion prior does not add significant information, making (10) applicable.

Fig. 2 shows the position error CDFs. It is evident that the channel characterization (red) yields excellent robustness, as all 25 runs have similar performance with $90\,\%$ of the errors below $4\,\mathrm{cm}$. Without SINR information (black/gray), the robustness is affected, as 10 of 25 runs diverge, mostly in the NLOS region discussed before. The overall CDF for the 15 non-diverging runs (black bold dashed line, circle markers) shows the *potential* performance of MINT without channel information, where $90\,\%$ of the errors are within $7\,\mathrm{cm}$. The influence of the MAP-re-localization of the VA positions (15) is illustrated by the CDF indicated by the blue dash-dotted curve with square markers. All runs are included, SINRs used, but without the re-localized VA positions. SINR awareness provides robustness, while re-localization improves accuracy.

Fig. 3 illustrates the mean number of associated MPCs,

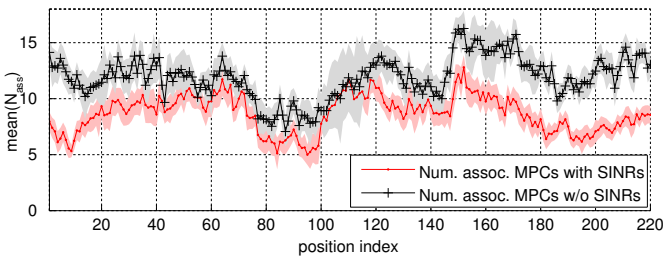

Fig. 3. Mean and standard deviation of the number of associated MPCs used for tracking. The 15 of 25 non-diverging runs are included for the case where no SINRs are available.

$\mathbb{E}\{|\mathcal{A}_{\ell,\mathrm{ass}}|\}$, over all runs using SINRs and the 15 non-diverging runs without SINRs, together with the standard deviation. The additional channel knowledge helps to substantially prune the set of potential VAs to the relevant ones. This leads to less erroneous associations of estimated MPCs to VAs and also reduces the computational complexity.

The results presented here match results in [11], which also includes quantitative results for the SINR estimation in different environments.

V. Conclusions

We have shown that channel knowledge quantifying the position-related information of deterministic MPCs is a key factor for obtaining accurate and robust indoor localization. By estimating the uncertainty of range estimates corresponding to deterministic MPCs and making this information available to a tracking filter, multipath propagation can be used efficiently. Experimental results have confirmed the advantage, demonstrating excellent performance.

References

[1] D. Dardari, A. Conti, U. Ferner, A. Giorgetti, and M. Z. Win, "Ranging With Ultrawide Bandwidth Signals in Multipath Environments," *Proceedings of the IEEE*, 2009.

[2] P. Meissner, E. Leitinger, M. Froehle, and K. Witrisal, "Accurate and Robust Indoor Localization Systems Using Ultra-wideband Signals," in *European Navigation Conference (ENC)*, Vienna, Austria, 2013.

[3] K. Witrisal and P. Meissner, "Performance bounds for multipath-assisted indoor navigation and tracking (MINT)," in *International Conference on Communications (ICC)*, Ottawa, Canada, 2012.

[4] P. Meissner and K. Witrisal, "Analysis of Position-Related Information in Measured UWB Indoor Channels," in *6th European Conference on Antennas and Propagation (EuCAP)*, Prague, Czech Repuplic, 2012.

[5] Y. Shen, S. Mazuelas, and M. Win, "Network Navigation: Theory and Interpretation," *IEEE Journal on Selected Areas in Communications*, 2012.

[6] A. Conti, D. Dardari, M. Guerra, L. Mucchi, and M. Win, "Experimental Characterization of Diversity Navigation," *IEEE Systems Journal*, 2014.

[7] N. Decarli, F. Guidi, and D. Dardari, "A Novel Joint RFID and Radar Sensor Network for Passive Localization: Design and Performance Bounds," *IEEE Journal of Selected Topics in Signal Processing*, 2014.

[8] J. Kunisch and J. Pamp, "An ultra-wideband space-variant multipath indoor radio channel model," in *IEEE Conference on Ultra Wideband Systems and Technologies*, 2003.

[9] D. Schuhmacher, B.-T. Vo, and B.-N. Vo, "A Consistent Metric for Performance Evaluation of Multi-Object Filters," *IEEE Transactions on Signal Processing*, 2008.

[10] Y. Shen and M. Z. Win, "Fundamental Limits of Wideband Localization - Part I: A General Framework," *IEEE Transactions on Information Theory*, Oct. 2010.

[11] P. Meissner, E. Leitinger, M. Lafer, and K. Witrisal, "Real-Time Demonstration System for Multipath-Assisted Indoor Navigation and Tracking (MINT)," in *IEEE ICC 2014 Workshop on Advances in Network Localization and Navigation (ANLN)*, Sydney, Australia, 2014.